The ubiquity of directional and reciprocating motion in enzymes out of equilibrium

David R. Slochower and Michael K. Gilson*

Skaggs School of Pharmacy and Pharmaceutical Sciences, University of California San Diego, La Jolla, California 92093-0736, United States

* mgilson@ucsd.edu

Summary paragraph

A biological molecular motor is an enzyme that uses the free energy of an out-of-equilibrium chemical reaction to drive mechanical motion. This motion must have a specific direction to fulfill the motor's functional role. For example, a corkscrew-shaped flagellum must rotate in the appropriate sense to propel the organism. The generation of directional motion appears to be a complex protein property, and it is not clear how the evolutionary leap from non-motor enzymes to molecular motors could have occurred. Indeed, the existence of biological molecular motors has been held up in the popular press as a mark against the theory of evolution[1]. Here, we provide evidence, based on atomistic simulations and kinetic modeling, that conformational switching of non-motor enzymes, induced by out-of-equilibrium substrate binding and catalysis, induces motor-like, directional torsional motions, as well as oar-like, reciprocating motions. Generalizing from these specific results, we provide an argument that virtually any chiral molecule undergoing conformational transitions out of equilibrium should be expected to undergo directional rotations on small and potentially large scales. Thus, the emergence of directional motion did not require an evolutionary leap. Instead, directional motion was present in the earliest enzymes, and only evolutionary optimization was needed for highly adapted motor proteins to emerge. Moreover, because chirality is a *sine qua non* for directional motion, the adaptive value of directional motors means that chirality itself is adaptive, so the need for directional motion may be one reason for the prevalence of chiral molecules in living systems. Finally, the ubiquity of driven molecular motions

in enzymes catalyzing reactions out of equilibrium might help explain why the diffusion constants of some enzymes increase with their catalytic rate [2-4].

27 **Text**

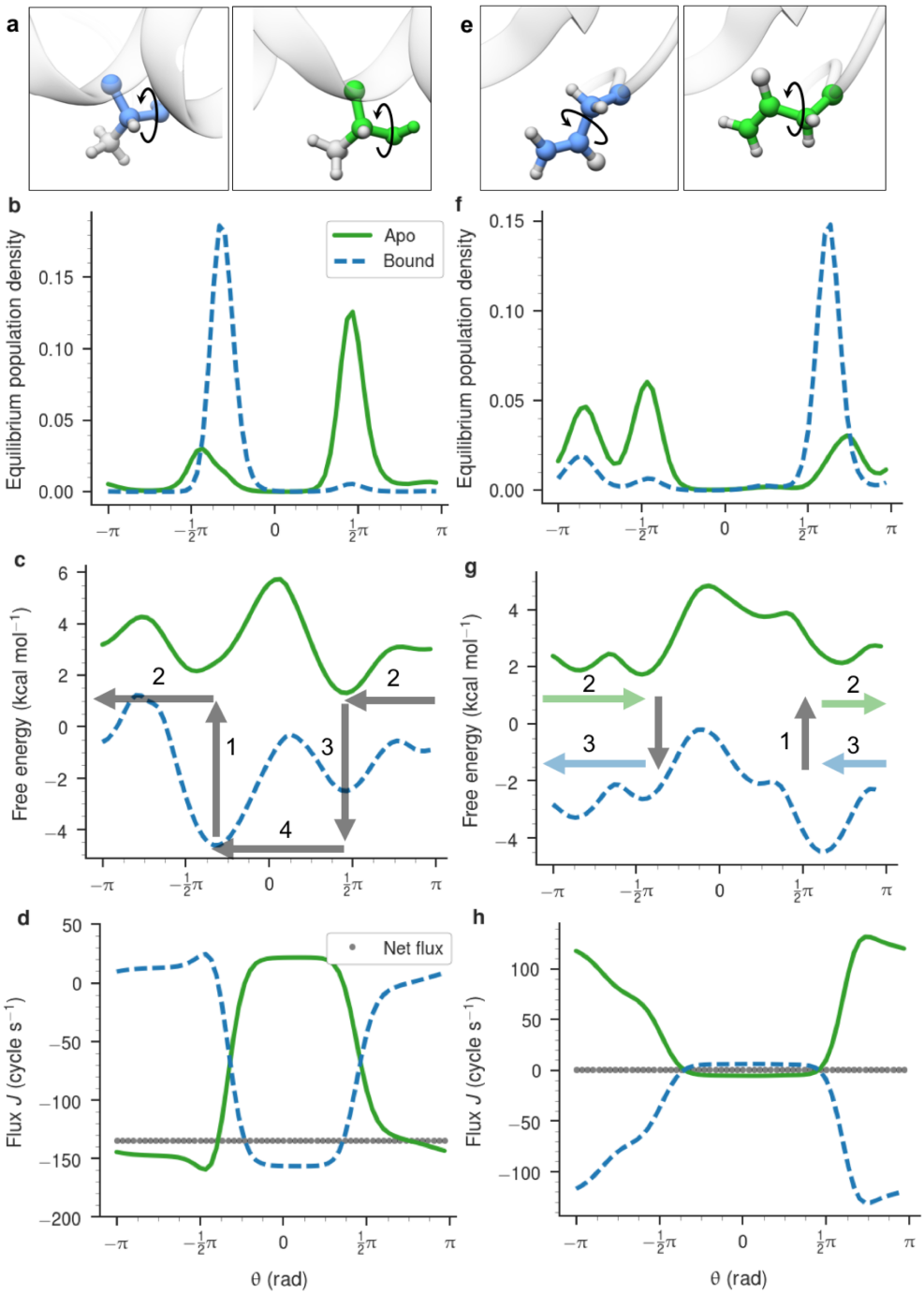

28

29 Figure 1. Protein torsion angles show directional and reciprocating motion. (a) ADK Thr175 in its crystallographic conformations
30 for the apo (green) and bound (blue) forms (see Supplementary Methods for PDB accessions) with the χ_2 angle denoted. The
31 coloring is the same for panels a through d. (b) Equilibrium population densities of this angle from MD simulations (Supplementary
32 Methods). (c) Free energy surfaces of this angle (Supplementary Methods) derived from the population densities in panel b. Arrows
33 indicate the direction of probability flux along, and between, the two surfaces. (d) The probability flux drawn separately for each
34 surface and as a sum (grey points), indicating large directional and reciprocating fluxes. (e-h) Same as a-d for ADK Asn138. In all
35 cases the substrate concentration is 10^{-3} M.

When any enzyme binds a molecule of substrate and catalyzes its conversion to product, it switches stochastically between two distinct conformational free energy surfaces, one for the apo state and one for the substrate-bound state. The flashing potential model[5-7], which has been used to understand the mechanisms of molecular motors[8-12], may be used to compute the dynamical consequences of this switching, given basic enzyme kinetic parameters and knowledge of the two energy surfaces. We computed the one-dimensional free energy surfaces of protein main- and side-chain torsions, discretized into bins, from detailed equilibrium molecular dynamics (MD) simulations of enzymes in their apo and substrate-bound states (Supplementary Methods). These data, coupled with literature values for the enzyme kinetic parameters (Supplementary Table 1), enabled us to define first order rate constants for transitions between neighboring bins on and between surfaces (Extended Data Fig. 1). The resulting set of rate equations was solved for the non-equilibrium steady state probability distribution across the surfaces. This, in turn, was used to compute the probability flux on each surface and the net flux, J, along both surfaces. Nonzero net flux implies directional rotation. We furthermore evaluated power output and performance under load by tilting the chemical potential surfaces to generate a torque, τ, opposite to the directional flux, which modifies the intrasurface bin-to-bin rate constants. The power output is the product of imposed torque and flux: $P = \tau J$. Both the maximum power and the stall torque, τ_{stall}, which brings the directional flux to zero, were found by scanning across values of applied torque.

We used this method to analyze motions in three enzymes, each with distinctive characteristics: adenylate kinase (ADK), with 214 residues and a relatively high k_{cat} ~300 s^{-1} [13,14], undergoes extensive conformational change on binding substrate, with two domains reorienting to form a compact conformation[15,16]; protein kinase A (PKA), with 350 residues and k_{cat} ~140 s^{-1} [17], acts as a "dynamic switch", with long-range allosteric interactions and domain rearrangement upon ligand

binding[18]; while HIV-1 protease (HIVP), with 200 residues and lower k_{cat} ~10 s^{-1} [19-21], contains two flexible flaps that lose mobility in the substrate-bound state[22,23] (Extended Data Fig. 2).

The present analysis indicates that torsions in all three enzymes exhibit directional torsional flux, driven by the catalytic conversion of substrate to product. The general mechanism by which directional flux is generated is illustrated by the χ_2 torsion of ADK Thr175 (Fig. 1a). This angle has a two-peaked probability distribution in both the bound and apo states, but the peak near $+\frac{\pi}{2}$ is favored in the apo state, while that near $-\frac{\pi}{2}$ is favored in the bound state (Fig. 1b,c). In the presence of substrate, the bound-state energy minimum near $-\frac{\pi}{2}$ is highly occupied (Fig. 1b,c). Catalytic breakdown of substrate pumps the system to the secondary energy minimum of the apo state at $-\frac{\pi}{2}$ (Fig. 1c, arrow 1). Probability then flows primarily to the left on the apo surface, because this is the lowest-barrier path to the apo state's global energy minimum near $+\frac{\pi}{2}$ (arrow 2; this flux goes through the periodic boundary at $\theta = -\pi \equiv +\pi$). Probability pooled in the global energy minimum of the apo state near $+\frac{\pi}{2}$, then flows primarily to the bound state, by binding substrate and landing in the secondary energy minimum of the bound state (arrow 3). It then flows back to the global minimum of the bound state via the lowest-barrier path, which is again leftward (arrow 4). The net effect is a leftward flux of up to -140 cycles s^{-1}. Fig. 1d shows the steady state flux on each surface: leftward flux predominates overall, but occurs on the apo surface between $-\frac{\pi}{2}$ to $+\frac{\pi}{2}$, and on the bound surface elsewhere, with crossovers between surfaces at the energy minima. This process parallels flashing potential mechanisms previously invoked to explain highly evolved molecular motors[7,8,11,12,24-27]. In the absence of significant directional flux, a torsion can still be actively driven back and forth between two angular ranges. For example, χ_2 of Asn 138 in

ADK (Fig. 1e) has essentially zero net flux but undergoes cycles of driven, reciprocating flux, with intrasurface fluxes reaching 130 cycles s^{-1} (Fig. 1d-h).

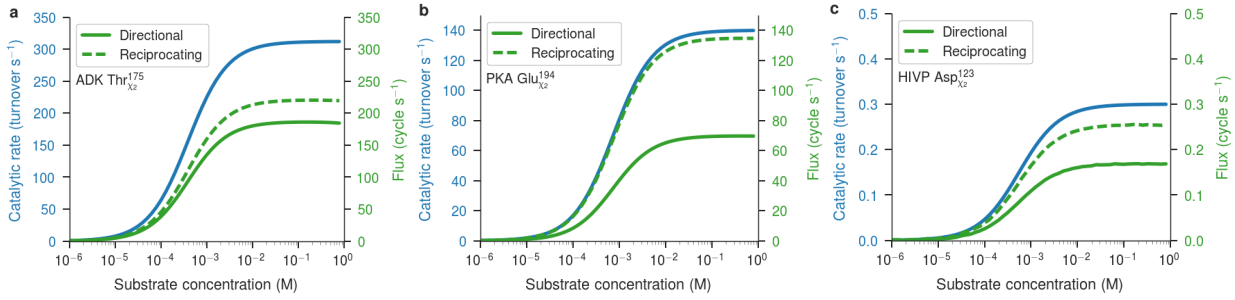

Figure 2. Dependence of catalytic rates and of the magnitudes of driven and directional fluxes on substrate concentration, for torsion angles in each enzyme. (a) The χ_2 angle of Thr175 in ADK reaches high levels of both directional and reciprocating flux. (b) The χ_2 angle of Glu194 in PKA reaches a high level of reciprocating flux and moderate level of directional flux. (c) Although the total amount of flux in the χ_2 angle of Asp123 in HIVP is low, the ratio of directional and reciprocating flux to the enzyme velocity is similar to that in ADK and PKA.

The fluxes are driven by catalytic breakdown of substrate: they are zero without substrate and rise sigmoidally with substrate concentration, along with the catalytic rate, as illustrated in Fig. 2 and Extended Data Fig. 3. Although the maximum directional fluxes in these examples are quite different for ADK, PKA and HIVP (180, 70 and 0.18 cycles s^{-1}, respectively), the ratios of flux to catalytic rate are similar, 0.5 – 0.6 cycles/catalytic turnover. This ratio is akin to a 2:1 gearing of catalysis to torsional rotation.

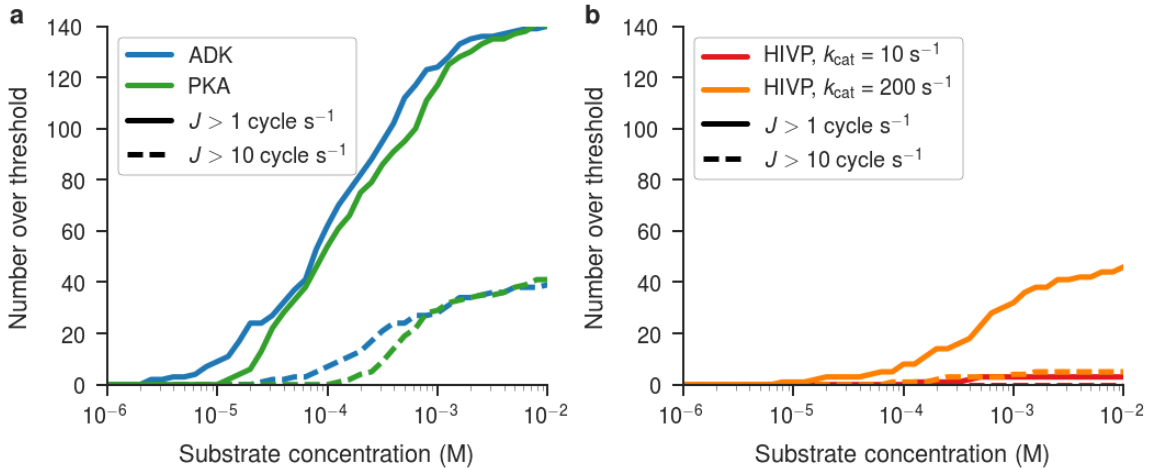

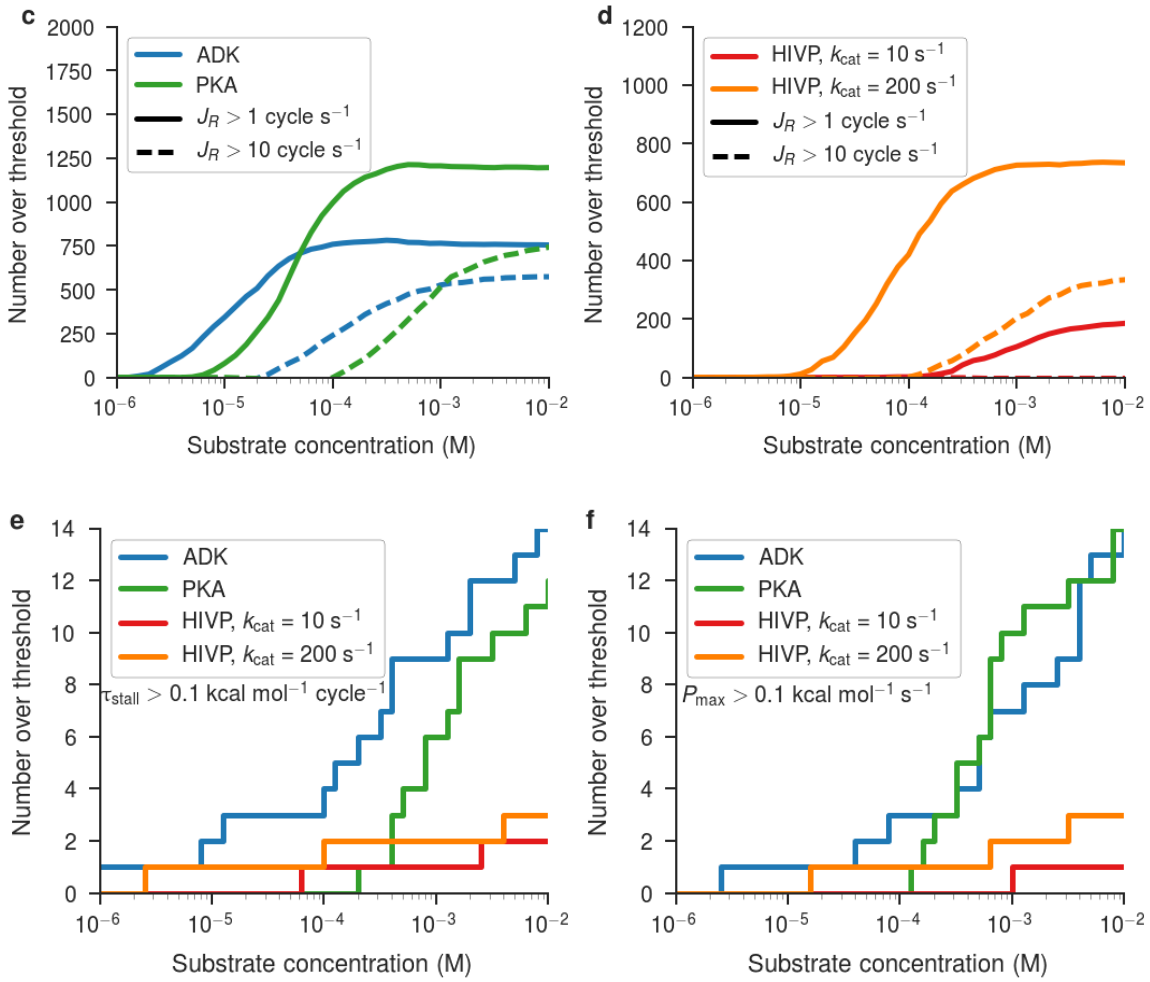

Figure 3. The number of torsions above various thresholds of directional flux magnitude, reciprocating flux magnitude, stall torque, and maximum power, as a function of substrate concentration. (a-b) The number of torsions with directional flux above 1 (solid) or 10 (dotted) cycle s^{-1} in ADK, PKA, and HIVP. (c-d) The number of torsions with reciprocating flux above 1 (solid) or 10 (dotted) cycle s^{-1} and, at the same time, directional flux less than 1 cycle s^{-1}. The number of angles with (e) maximum stall force above 0.1 kcal/(mol·cycle) and (f) power above 0.1 kcal/(mol·s^{-1}).

In addition to torsions with fluxes that approach the catalytic rate, each enzyme also has many torsions with a lower but definite directional or reciprocating flux. Thus, at high substrate concentration, about 40 torsions in ADK are found to rotate faster than 10 cycle s^{-1}, and about 140 are found to rotate faster than 1 cycle s^{-1} (Fig. 3a). The corresponding numbers are lower for HIVP (Fig. 3b, red). This largely reflects the lower k_{cat} value of HIVP, about 10 s^{-1} [19-21] compared with 200-300 s^{-1} for PKA[17,28] and ADK[13,14]. Thus, artificially assigning $k_{cat} = 200\ s^{-1}$ to HIVP leads to substantial increases in the number of torsions with fluxes of at least 10 s^{-1} and at least 1 s^{-1} (Fig.

3b, orange and Extended Data Fig. 4). This means that many of the torsional PDFs in HIVP generate low fluxes primarily because k_{cat} is low for this enzyme. The tendency toward lower fluxes in HIVP may also reflect the smaller scale of its conformational changes (Extended Data Fig. 2). In addition to torsions with net directional flux >0.1 cycles s^{-1}, many torsions are predicted to undergo large reciprocating fluxes. Indeed, ADK and PKA are predicted to have ~1250 and ~750 torsions whose reciprocating motions occur at rates of at least 1 cycle s^{-1} with minimal concomitant directional flux (Fig. 3c,d). These angles are distributed throughout the proteins, with high flux torsions localized near the substrate binding pocket or mobile regions (Extended Data Fig. 2).

The directional torsions in these enzymes can do work against small mechanical loads and thus generate power (Fig. 3e,f). At high substrate concentrations, torsions in ADK and PKA are predicted to generate stall torques up to 2.4 and 1.6 kcal mol^{-1} $cycle^{-1}$, respectively, and maximum power outputs per torsion of 70 and 28 kcal mol^{-1} s^{-1}.

Directional flux can be generated only by a chiral molecule. Otherwise, the energy surfaces of the torsions would not distinguish between flux to the right (e.g., clockwise) and flux to the left (counterclockwise), so there would be no physical basis for net motion in one direction. Indeed, as illustrated in the Extended Data Fig. 5, artificially symmetrizing the energy surfaces of a torsion angle abolishes directional flux, though substantial reciprocating fluxes can remain.

The central result of this study is that enzymes not normally regarded as motor proteins can have motor-like properties: in the presence of excess substrate, they exhibit not only driven reciprocating motions but also directional rotation. Furthermore, the specific findings for ADK, PKA, and HIVP may be generalized by a simple physical argument based on the same flashing potential kinetic model. Consider any chiral molecule with a degree of freedom that is switched

back and forth between two energy surfaces. After the energy surface is switched, the asymmetry of the new energy surface means that probability will, in net, flow more in one direction than the other. When the surface is switched back, a second directional probability flow occurs, this time on the other energy surface, and only by coincidence will the two probability flows cancel perfectly, unless a large energy barrier entirely blocks circular motion. The imbalance between the two flows represents directional flux.

Although this study focuses on torsional motions, the same physical reasoning applies to larger scale conformational motions, so directional motions in enzymes catalyzing reactions out of equilibrium likely also involve motions through higher-order conformational subspaces. For example, the concerted opening and closing of an active site could occur along two different paths, thus exhibiting hysteretic cycling. Such concerted motions might be stronger, in terms of force and power, than the torsional motions studied here, and their hydrodynamic coupling with solvent might help explain why some enzymes diffuse faster when catalytically active[2-4,29,30]. We note that, despite the scallop theorem[31], driven reciprocating motions could also speed enzyme diffusion if they occur on time scales slower than the rotational diffusion of the enzyme, which is typically about 10-100 ns, because then the forward and reverse translations would have different directions.

Thus, an enzyme catalyzing a reaction out of equilibrium can undergo directional probability flows through multiple conformational cycles, as well as driven reciprocating motions. Such motions could have been the starting points for the evolution of today's efficient motor proteins, and might also provide toeholds for *in vitro* directed evolution of mechanically active enzymes. Additionally, because directional motion requires chirality, the adaptive advantages of directional motor proteins, such as in flagellar propulsion, could be one reason that natural selection led to biomolecules that are chiral.

Methods

Methods, including statements of data availability and any associated accession codes and references, are available in the online version of the paper. The datasets generated and analyzed during the current study are available in the GitHub repository https://github.com/GilsonLabUCSD/nonequilibrium.

Code availability

The Python code used to analyze the simulation data and implement the kinetic model is available at the same GitHub repository.

Acknowledgements

We thank Dr. N.-L. Huang for assistance preparing simulations on ADK and HIVP, and Drs. A. Gilson, K. Lindenberg, C. Van den Broeck, and J.A. McCammon for theoretical discussions. This work was funded in part by grant GM061300 from the National Institutes of Health (NIH). Its contents are solely the responsibility of the authors and do not necessarily represent the official views of the NIH.

Author Contributions

M.K.G. conceived and designed the project. D.R.S. implemented the model and performed the simulations. M.K.G. and D.R.S. analyzed the data and wrote the manuscript.

Author Information

MKG has an equity interest in and is a cofounder and scientific advisor of VeraChem, LLC.

References

1 Pallen, M. J. & Matzke, N. J. From The Origin of Species to the origin of bacterial flagella. *Nat. Rev. Microbiol.* **4**, 784-790, doi:10.1038/nrmicro1493 (2006).

2 Muddana, H. S., Sengupta, S., Mallouk, T. E., Sen, A. & Butler, P. J. Substrate catalysis enhances single-enzyme diffusion. *J. Am. Chem. Soc.* **132**, 2110-2111, doi:10.1021/ja908773a (2010).

3 Sengupta, S. *et al.* Enzyme molecules as nanomotors. *J. Am. Chem. Soc.* **135**, 1406-1414, doi:10.1021/ja3091615 (2013).

4 Riedel, C. *et al.* The heat released during catalytic turnover enhances the diffusion of an enzyme. *Nature* **517**, 227-230, doi:10.1038/nature14043 (2015).

5 Astumian, R. D. Thermodynamics and kinetics of a Brownian motor. *Science* **276**, 917-922 (1997).

6 Astumian, R. D. & Bier, M. Fluctuation driven ratchets: Molecular motors. *Phys Rev Lett* **72**, 1766-1769, doi:10.1103/PhysRevLett.72.1766 (1994).

7 Kay, E. R., Leigh, D. A. & Zerbetto, F. Synthetic molecular motors and mechanical machines. *Angew Chem Int Ed Engl* **46**, 72-191, doi:10.1002/anie.200504313 (2007).

8 Wang, H. & Oster, G. Ratchets, power strokes, and molecular motors. *Applied Physics A* **75**, 315-323, doi:10.1007/s003390201340 (2002).

9 Astumian, R. D. Optical vs. chemical driving for molecular machines. *Faraday Discuss.*, doi:10.1039/c6fd00140h (2016).

198 10 Astumian, R. D. Stochastic conformational pumping: a mechanism for free-energy
199 transduction by molecules. *Annu Rev Biophys* **40**, 289-313, doi:10.1146/annurev-biophys-
200 042910-155355 (2011).
201 11 Astumian, R. D. Enhanced diffusion, chemotaxis, and pumping by active enzymes:
202 progress toward an organizing principle of molecular machines. *ACS Nano* **8**, 11917-
203 11924, doi:10.1021/nn507039b (2014).
204 12 Riemann, P. Brownian motors: noisy transport far from equilibrium. *Physics Reports*
205 (2002).
206 13 Aden, J., Verma, A., Schug, A. & Wolf-Watz, M. Modulation of a Pre-existing
207 Conformational Equilibrium Tunes Adenylate Kinase Activity. *J. Am. Chem. Soc.* **134**,
208 16562-16570, doi:10.1021/ja3032482 (2012).
209 14 Wolf-Watz, M. *et al.* Linkage between dynamics and catalysis in a thermophilic-
210 mesophilic enzyme pair. *Nat. Struct. Mol. Biol.* **11**, 945-949, doi:10.1038/nsmb821 (2004).
211 15 Gerstein, M., Schulz, G. & Chothia, C. Domain closure in adenylate kinase. Joints on either
212 side of two helices close like neighboring fingers. *J. Mol. Biol.* **229**, 494-501,
213 doi:10.1006/jmbi.1993.1048 (1993).
214 16 Hanson, J. A. *et al.* Illuminating the mechanistic roles of enzyme conformational dynamics.
215 *Proc Natl Acad Sci U S A* **104**, 18055-18060, doi:10.1073/pnas.0708600104 (2007).
216 17 Adams, J. A. Kinetic and catalytic mechanisms of protein kinases. *Chem Rev* **101**, 2271-
217 2290 (2001).
218 18 McClendon, C. L., Kornev, A. P., Gilson, M. K. & Taylor, S. S. Dynamic architecture of
219 a protein kinase. *Proc Natl Acad Sci U S A* **111**, E4623-4631,
220 doi:10.1073/pnas.1418402111 (2014).

19 Wondrak, E. M., Louis, J. M. & Oroszlan, S. The Effect of Salt on the Michaelis Menten Constant of the Hiv-1 Protease Correlates with the Hofmeister Series. *FEBS Lett.* **280**, 344-346, doi:Doi 10.1016/0014-5793(91)80327-Y (1991).

20 Windsor, I. W. & Raines, R. T. Fluorogenic Assay for Inhibitors of HIV-1 Protease with Sub-picomolar Affinity. *Sci Rep* **5**, 11286, doi:10.1038/srep11286 (2015).

21 Pokorna, J., Heyda, J. & Konvalinka, J. Ion specific effects of alkali cations on the catalytic activity of HIV-1 protease. *Faraday Discuss* **160**, 359-370; discussion 389-403 (2013).

22 Scott, W. R. P. & Schiffer, C. A. Curling of Flap Tips in HIV-1 Protease as a Mechanism for Substrate Entry and Tolerance of Drug Resistance. *Structure* **8**, 1259-1265, doi:10.1016/S0969-2126(00)00537-2 (2000).

23 Kurt, N., Scott, W. R. P., Schiffer, C. A. & Haliloglu, T. Cooperative fluctuations of unliganded and substrate-bound HIV-1 protease: A structure-based analysis on a variety of conformations from crystallography and molecular dynamics simulations. *Proteins* **51**, 409-422, doi:10.1002/prot.10350 (2003).

24 Coskun, A., Banaszak, M., Astumian, R. D., Stoddart, J. F. & Grzybowski, B. A. Great expectations: can artificial molecular machines deliver on their promise? *Chem Soc Rev* **41**, 19-30, doi:10.1039/c1cs15262a (2012).

25 Howard, J. Motor Proteins as Nanomachines: The Roles of Thermal Fluctuations in Generating Force and Motion. *Seminaire Poincare* (2009).

26 Bustamante, C., Keller, D. & Oster, G. The physics of molecular motors. *Acc Chem Res* **34**, 412-420 (2001).

27 Keller, D. & Bustamante, C. The mechanochemistry of molecular motors. *Biophys. J.* **78**, 541-556, doi:10.1016/S0006-3495(00)76615-X (2000).

28 Shaffer, J. & Adams, J. A. An ATP-linked structural change in protein kinase A precedes phosphoryl transfer under physiological magnesium concentrations. *Biochemistry* **38**, 5572-5581, doi:10.1021/bi982768q (1999).

29 Bai, X. & Wolynes, P. G. On the hydrodynamics of swimming enzymes. *J Chem Phys* **143**, 165101, doi:10.1063/1.4933424 (2015).

30 Hwang, W. & Hyeon, C. Quantifying the Heat Dissipation from a Molecular Motor's Transport Properties in Nonequilibrium Steady States. *J Phys Chem Lett* **8**, 250-256, doi:10.1021/acs.jpclett.6b02657 (2017).

31 Purcell, E. M. Life at Low Reynolds-Number. *American Journal of Physics* **45**, 3-11, doi:Doi 10.1119/1.10903 (1977).